Iran J Pharm Res. 2022 December; 21(1):e127000. doi: 10.5812/ijpr-127000.

Published online 2022 August 28. **Research Article**

Icariin Exerts Estrogen-Like Actions on Proliferation of Osteoblasts in Vitro via Membrane Estrogen Receptors-Mediated Non-nuclear Effects

Dapeng Zhang [1, 2], Yan Su [3], Qiang He [1, 2], Yajie Zhang [4], Ning Gu [5], Xu Zhang [6], Kun Yan [1, 2], Nianwei Yao [1] and Weiqing Qian [1, *]

[1] Department of Orthopedics, Nanjing Hospital of Chinese Medicine Affiliated to Nanjing University of Chinese Medicine, Nanjing, 210022, Jiangsu, P.R. China
[2] Nanjing University of Chinese Medicine, Nanjing, 210023, Jiangsu, P.R. China
[3] Reproductive Center, Obstetrics and Gynecology Hospital Affiliated to Nanjing Medical University, Nanjing, 210029, Jiangsu, P.R. China
[4] Central Laboratory, Nanjing Hospital of Chinese Medicine Affiliated to Nanjing University of Chinese Medicine, Nanjing, 210022, Jiangsu, P.R. China
[5] Department of Cardiovascular Medicine, Nanjing Hospital of Chinese Medicine Affiliated to Nanjing University of Chinese Medicine, Nanjing, 210022, Jiangsu, P.R. China
[6] School of Medicine and Life Sciences, Nanjing University of Chinese Medicine, Nanjing, 210023, Jiangsu, P.R. China

[*] *Corresponding author*: Department of Orthopedics, Nanjing Hospital of Chinese Medicine Affiliated to Nanjing University of Chinese Medicine, Nanjing, 210022, Jiangsu, P.R. China. Email: qwq68@126.com

Received 2022 April 16; **Revised** 2022 July 25; **Accepted** 2022 July 26.

Abstract

Background: According to reports, icariin (ICA) is a bone anabolic agent able to prevent osteoporosis in both ovariectomized rats and postmenopausal women. However, its effect on osteoblast proliferation remains to be determined, and the underlying mechanism remains to be elucidated.

Methods: Icariin-bovine serum albumin (BSA) conjugates were purified by Sephadex G-25 gel chromatography technology. Primary osteoblasts from neonatal rats were used to evaluate the effects of ICA, ICA-BSA, ICA-BSA + ICI182780, and ICA-BSA + PD98059. 3-(4,5-dimethyl-thiazol-2-yl)-2,5-diphenyl tetrazolium bromide (MTT) and propidium iodide (PI)-staining assays were used to detect the proliferation of osteoblasts after drug exposure. The intracellular calcium ions were detected using a confocal microscope with Fluo-3/AM as the fluorescent indicator. Western blot was capitalized on to measure the relative content of phospho-extracellular signal-regulated kinase (p-ERK).

Results: Primary osteoblasts in culture were detected by histochemical staining of alkaline phosphatase, and calcified nodules were obtained by sequential digestion. Icariin and bovine serum albumin could form conjugate, which could be purified by Sephadex G-25 gel chromatography technology. MTT and flow cytometry results show that ICA-BSA conjugate significantly facilitated the proliferation of osteoblasts ($P < 0.05$). The intracellular calcium ions also ascended vastly in the cells treated with ICA-BSA conjugate ($P < 0.01$). Icariin-bovine serum albumin exposure rapidly activated the extracellular signal-regulated kinase (ERK) signaling. Furthermore, ICA- and ICA-BSA-mediated actions on osteoblasts were signally alleviated after dealing with ERK inhibitor PD98059 or estrogen receptor (ER) antagonist ICI182780, which might have a relation to the repression of ERK phosphorylation.

Conclusions: Icariin could serve as estrogen in osteoblast cells by the rapid nongenomic ER signaling pathway independent of ligand and estrogen response element (ERE) and mediated by mitogen-activated protein kinase (MAPK).

Keywords: Icariin, Osteoblasts, Non-nuclear Effects, Cell Proliferation

1. Background

Osteoporosis, a systemic bone disease, is characterized by low bone mass and bone microstructure damage (1), resulting in increased bone fragility and susceptibility to fracture. It has caused widespread medical attention due to the economic and social burdens it brings to patients' attention (2). At present, drugs widely used for osteoporosis treatment mainly exert the biological effect of impeding bone resorption, but they can also cause osteonecrosis (3). To reduce the bone loss, osteoblasts should be induced for bone reconstruction. In addition to the approved anabolic agents for osteoporosis (including parathyroid hormone (PTH), calcium-sensitive receptor (CaSR) antagonists, and antibodies against Wnt signaling inhibitor) (4, 5), isoflavones have shown their clinical promise in preventing osteoporosis (6).

Icariin (ICA), the main bioactive flavonoid glycoside isolated from a traditional Chinese medicine named *Epimedium* (HEF) (7), has a similar structure to estradiol and can perform as a bone anabolic agent. Moreover, it has been reported that icariin treatment could prevent osteoporosis in both ovariectomized rats and postmenopausal

women. In recent years, phytoestrogens, polyphenolic non-steroidal compounds derived from plants, have shown estrogen-like biological activity. Their application in treating menopausal-related diseases and postmenopausal osteoporosis has attracted widespread attention in the medical community (8-10). According to reports, icariin can effectively inhibit the bone loss induced by ovariectomy (OVX), and promote the proliferation, differentiation, osteoprotegerin (OPG) expression, and alkaline phosphatase activity of primary osteoblasts. In our previous study, we demonstrated that icariin extract effectively promotes the proliferation and differentiation of osteoblasts at the concentration of 10 micrograms/liter (11). However, whether icariin has an estrogen-like effect and the mechanism underlying this effect remains to be determined.

As a family of secondary messengers, mitogen-activated protein kinases (MAPKs) can serve as the medium for transmitting signals to the nucleus from the cell surface in responding to various stimuli like hormones, chemicals, and stress (12). The MAPK/extracellular signal-regulated kinases (ERK) signal cascade regulates the expression of genes correlated with mitosis, proliferation, differentiation, and apoptosis (7). Extracellular signal-regulated kinase signaling in osteoblasts can be activated by many bone-active agents, such as platelet-derived growth factor (PDGF), fibroblast growth factor (FGF), and estrogen (13, 14).

2. Objectives

Considering the similar structure of icariin and estrogen, we hypothesized that icariin plays the same role as phytoestrogens in bones. In the present study, the role of icariin in the proliferation of cells was evaluated in detail, and the role of ERK signaling in this process was determined.

3. Methods

3.1. Animal Experiments

Neonatal Sprague-Dawley (SD) rats (clean grade) were bought from the Experimental Animal Center of the Nanjing University of Chinese Medicine. The animal study was checked and approved by the Animal Care Committee of the Nanjing University of Chinese Medicine and performed as per the Declaration of the National Institutes of Health Guide for Care and Use of Laboratory Animals (NIH publication NO.85-23, revised 1996). The rats were put in feeding boxes at 19 - 27°C, with a humidity of 45% - 75%, noise level below 85 decibels, ammonia concentration below 20 ppm, and ventilation 8 - 12 times per hour. Ensure a sufficient amount of fresh and dry feed in feeding hoppers.

3.2. Chemicals

Icariin (CAS No: 489-32-7) with the purity of more than 98 % and 3-(4,5-dimethyl-thiazol-2-yl)-2,5-diphenyl tetrazolium bromide (MTT) were acquired from Sigma-Aldrich (Saint Louis, USA) through a financial transaction. PD98059 and ICI182780 were separately acquired from Beyotime Biotechnology (Shanghai, China) and Dalian Meilun Biotech Co., Ltd. (Dalian, China) through a financial transaction.

3.3. The Interaction Between Icariin and Bovine Serum Albumin

The ICA stocking solution (5×10^{-5} mol/L) was prepared by dissociating PBS (pH = 7.40, Thermo Fisher Scientific, USA). The bovine serum albumin (BSA) stocking solution was prepared by dissociating PBS (pH = 7.40). To prepare ICA-BSA working solution, 100 μL ICA stocking solution, 100 μL 5×10^{-5} mol/L BSA (Sigma-Aldrich, USA) diluted in PBS (pH = 7.40), 1 mL 0.1 mol/L Tris-HCl solution and 2.8 mL deionized water were mixed in the test tube. Then ICA-BSA working solution was incubated at different temperatures (17°C, 27°C, and 37°C, respectively) and shocked for 10 min. The ICA working solution (1.25×10^{-6} mol/L) was prepared by mixing 100 μL ICA stocking solution, 1 mL 0.1 mol/L, and 2.9 mL deionized water. The BSA working solution (1.25×10^{-6} mol/L) was prepared by mixing 100 μL BSA stocking solution, 1 mL 0.1 mol/L Tris-HCl solution, and 2.9 mL deionized water. To determine the fluorescence emission peak of ICA-BSA conjugates, 200 μL ICA-, BSA-, and ICA-BSA working solutions were added into the 96-well plates, and the OD values in the wavelength range of 200 - 500 nm were acquired with a microplate reader, respectively. For each experiment solution, preparation was conducted in triplicate, and the average value was taken to draw the absorbance curve to determine whether the ICA-BSA conjugate was formed. Finally, the ICA-BSA conjugates were purified by chromatography with Sephadex G-25 column (Sheng Xing Biological Technology, China).

3.4. Primary Calvarial Osteoblasts Purification and Culture

Excised calvariae (frontal and parietal bones) from neonatal SD rats were digested with a sequential enzyme to acquire primary rat osteoblasts. Briefly, the periosteal layers on both sides were carefully stripped off with tweezers under PBS. Then the calvariae were transferred to Petri dishes and incubated with 0.25% trypsin with ethylene diamine tetraacetic acid disodium (trypsin-EDTA, Gibco, USA) and 0.1% collagenase II (Sigma-Aldrich, USA) successively. After discarding the first two digests, the cells were

harvested from the final digest, followed by resuspension in Dulbecco's Modified Eagle Medium (DMEM, Gibco, USA) supplemented with 10% fetal bovine serum (FBS, Gibco, USA) and penicillin/streptomycin (Gibco, USA) in a humidified atmosphere with 5% CO_2 at 37°C. They were then cultivated at 37°C in a CO_2 (5%) incubator in a humidified atmosphere for 2 - 4 days until confluent (1 calvarial bone/flask). Primary osteoblast cells were identified by alkaline phosphatase (ALP, Beyotime Biotechnology, Shanghai, China) staining and calcified nodules staining. Alkaline phosphatase activity assay kit was used to identify ALP activity of cell culture medium. The operation procedures refer to the kit manual. Calcified nodules were detected using alizarin red staining.

3.5. Drug Treatment and MTT Assay

Osteoblast cells were assigned into four groups, including Group A (ICA), Group B (ICA-BSA), Group C (ICA-BSA + ICI182780), and Group D (ICA-BSA + PD98059). After 48 h of seeding in a 96-well plate at 2.5×10^4 cells/well in 200 μL of culture medium, osteoblast cells in Group C and Group D were separately incubated with culture media containing 1 μmol/L ICI18278 for 1 hour, and culture media containing 50 μmol/L PD98059 for 1 hour. Then the cells in Group A were added with 10 μg/L icariin. In some experiments, cells in Group B, C, and D were processed with 10 μg/L ICA-BSA. After this, an MTT assay was accomplished to determine the viability of osteoblasts in each group. Briefly, after washing with PBS once, the cells were subjected to 4 h of cultivation (at 37°C) with 20 μL MTT solution (5 mg/mL). The precipitated formazan subsequently underwent dissolution in dimethyl sulfoxide. The absorbance value at 490 nm was recorded with a microplate reader (Becton Dickinson, Mountain View, CA).

3.6. Flow Cytometry

The cell cycle distribution of cells with different treatments was determined by flow cytometry. Osteoblast cells were grouped as described above and then inoculated in a 96-well plate at 1.0×10^5 cells/well in 200 μL of culture medium. Following incubation with drugs, the cells were dissociated with 0.25% trypsin without EDTA (Gibco, USA), and FBS was used to stop trypsin activity. After being centrifuged at 1000 g for 4 min, the supernatant was discarded. The cells were resuspended in PBS solution, followed by 1 h of fixation with ice-cold 70% ethanol, washing with PBS again, and 30 min of incubation (at 37°C) with 1 mg/mL RNase A (Sigma-Aldrich, USA). After that, they experienced suspension in 0.5 mL of propidium iodide (PI)/RNase Staining Buffer, followed by 15 min incubation at room temperature. Afterward, a FACS Calibur cytometer (Becton Dickinson, Mountain View, CA) was adopted to analyze stained cells. CELLQuest 3.3 software (Becton Dickinson, Mountain View, CA) was employed to acquire samples at a low flow rate, and ModFit LT 2.0 software (Verity Software House, Topsham, ME) was utilized for analyzing list mode data. Three independently repeated experiments were conducted.

3.7. Western Blot Analysis

Western blot analysis was employed to determine protein expressions in cells from different treatments. The cells scraped down were lysed in radioimmunoprecipitation (RIPA) lysis buffer on ice for 25 min, followed by a 5 min centrifugation at 13,000 g for clarification and then protein harvest. After that, measurement of protein concentration was implemented utilizing a bicinchoninic acid (BCA) kit (Beyotime Biotechnology, China). A total of 40 μg of cellular protein extract was electrophoresed via 8% sodium dodecyl sulfate-polyacrylamide gel electrophoresis (SDS-PAGE) and moved onto polyvinylidene difluoride membranes (PVDF; Beyotime Biotechnology, China), followed by 3 h of membrane incubation (at room temperature) with blocking buffer comprising Tris-buffered saline and Tween 20 (TBST, 0.1% Tween 20) and 5% non-fat dry milk. After that, membrane rinsing was done twice with TBST for 15 min, followed by membrane incubation with primary antibodies against ERK1/2, phosphor (p)-ERK 1/2, and α-tubulin overnight at 4°C. The membrane washing was then conducted with TBST (0.05% Tween 20) three times (10 min each), followed by 1 h of cultivation (at room temperature) with secondary horseradish peroxidase (HRP)-conjugated antibody (1: 1000 in 1% milk, 1% BSA in TBST). After that, TBST was employed for repeated membrane washing. The membranes were detected using an enhanced chemiluminescence (ECL) kit, followed by visualization using the Lumi-Imager with Lumi Analyst version 3.10 software (Roche, Germany).

3.8. Determination of Intracellular Calcium Ions by Fluo-3/AM

Laser scanning confocal microscopy (LSCM) technology and Fluo-3/AM were used to determine the variation of intracellular calcium ions in each group. Cells (5×10^5) were incubated with 6 mL DMEM having 10% FBS (Gibco, USA) as a component under the following conditions: Humidified atmosphere, 5% CO_2, and 37°C in the absence or presence of 200 μL ICI18278 (1 μmol/L, Group C) or 200 μL PD98059 (50 μmol/L, Group D) for 1 hour. After that, 200 μL Fluo-3/AM (5 μmol/L) were directly added into the medium, followed by an additional 1 h incubation at the same condition. After that, sample washing was carried out twice with PBS. Finally, the samples treated with ICA (Group A), ICA-BSA (Group B), and Group C and D were evaluated in

the LSCM at 488 nm excitation and detected at 493 - 620 nm emission. Further graphical analysis was conducted to discuss the mechanism of the abirritation of icariin. Results of three independent experiments were averaged.

3.9. Statistical Analysis

The statistical analysis was done using the SPSS software (version 21.00, IBM, USA) and Prism software (version 8.0, GraphPad Software, San Diego, CA). Data were indicated through mean ± SEM. The comparisons among the different groups (> 2 groups) were analyzed by one-way ANOVA and Tukey's post hoc test, while Student's *t*-test was used for comparisons between 2 groups.

4. Results

4.1. Characterization of Primary Osteoblastic Cells in Culture

Osteoblasts were isolated from rat skull and showed adherent growth after one day of culture and showed the morphology of fusiform or polygonal, and gradually reached a confluence of 80%. The osteoblasts were identified by histochemical staining of alkaline phosphatase and calcified nodules (Figure 1). The active sites of alkaline phosphatase were shown as gray-black granules in the cell cytoplasm (Figure 1A - C). The black trabecular-shaped mineralized bone nodules formed by cells were also observed (Figure 1D – F). Furthermore, after alizarin red S staining, the mineralization of the culture is dark brown in the middle and light orange in the periphery (Figure 1G – I). Therefore, bone cells could be obtained by sequential digestion, and the osteoblast cells in culture could be identified by histochemical staining of alkaline phosphatase and calcified nodules.

4.2. Sephadex G-25 Chromatography Results

To obtain the ICA-BSA conjugate, we collected 2 mL liquid from the bottom of chromatography using tubes numbered 1 to 12. The Ultraviolet (UV)-visible absorbance values were determined at the wavelength ranging from 200 nm to 350 nm (Table 1). The sample in tube No. 4 displayed the highest UV-visible absorbance values, especially at 300 nm and 310 nm (Figure 2A). Since a strong fluorescence emission peak is observed at 305 nm in ICA-BSA, we considered that the ICA-BSA conjugate was mainly concentrated in tube No. 4, which was used for subsequent experiments. The UV absorbance of the standard curve of ICA-BSA protein was determined by BCA assay (Figure 2B), and the concentration of ICA-BSA conjugate was calculated as 60.5 μg/mL.

4.3. Icariin Promotes Osteoblast Proliferation

To determine the effect of ICA on osteoblast proliferation, MTT cell viability assay was performed, and osteoblast viability was significantly increased after ICA-BSA treatment compared to other control groups (Figure 3A, Table 2). MTT of group A was also remarkably different from that of groups C and D ($P < 0.05$), while it was comparable between groups C and D.

4.4. Cell Cycle Progression Measured by Flow Cytometry

To determine the impression of ICA on the cell cycle process, we performed flow cytometry analysis and found that treated osteoblast with ICA-BSA displayed a substantially elevated number of cells in S and G2/M phases in comparison to the other groups, manifesting that ICA-BSA appeared to boost cell cycle process (Figure 3B). Quantitatively, the percentage of S + G2 phase in the ICA and ICA-BSA groups was 26.13 ± 1.06 and 31.71 ± 0.65%, respectively, which was significantly higher than that in the C group and D group, and the difference was statistically significant (Table 3), while such a percentage was comparable between groups C and D ($P > 0.05$). The above results implied that ICA treatment can speed up cell cycle progression, thus presumably boosting the proliferation and stemming the apoptosis of cells.

4.5. Icariin Activates Extracellular Signal-Regulated Kinase Pathways in Osteoblasts

To determine whether the MAPK signaling pathway was activated in osteoblast cells after exposure to icariin, we performed a western blot analysis and found that ICA-BSA treatment significantly induced phosphorylation of ERK when compared to the other control group (Figure 3C and D). The addition of p-MEK1 inhibitor PD98059 and estrogen inhibitors ICI182780 significantly suppressed ICA-induced ERK phosphorylation. These data signified that ERK signaling participated in the icariin-induced proliferation of osteoblasts. Since icariin can elevate the circulating level of estradiol in ovariectomized rats and prevent bone loss in ovariectomized rats and postmenopausal women, we hypothesized that the estrogen receptor signaling pathway might be downstream of icariin stimulus. Therefore, we evaluated the role of the estrogen receptor inhibitor ICI182780 in ICA and ICA-BSA-induced osteoblast differentiation. The stimulatory effects of icariin were significantly attenuated by ICI182780. Besides, the ERK activation by icariin was also inhibited by ICI182780, so the role was partially managed through MAPK signaling (Table 4). Furthermore, icariin-triggered osteoblast mineralization was also attenuated by ICI182780, illustrating that membrane estrogen receptor signaling was also a player in the anabolic action mediated by icariin.

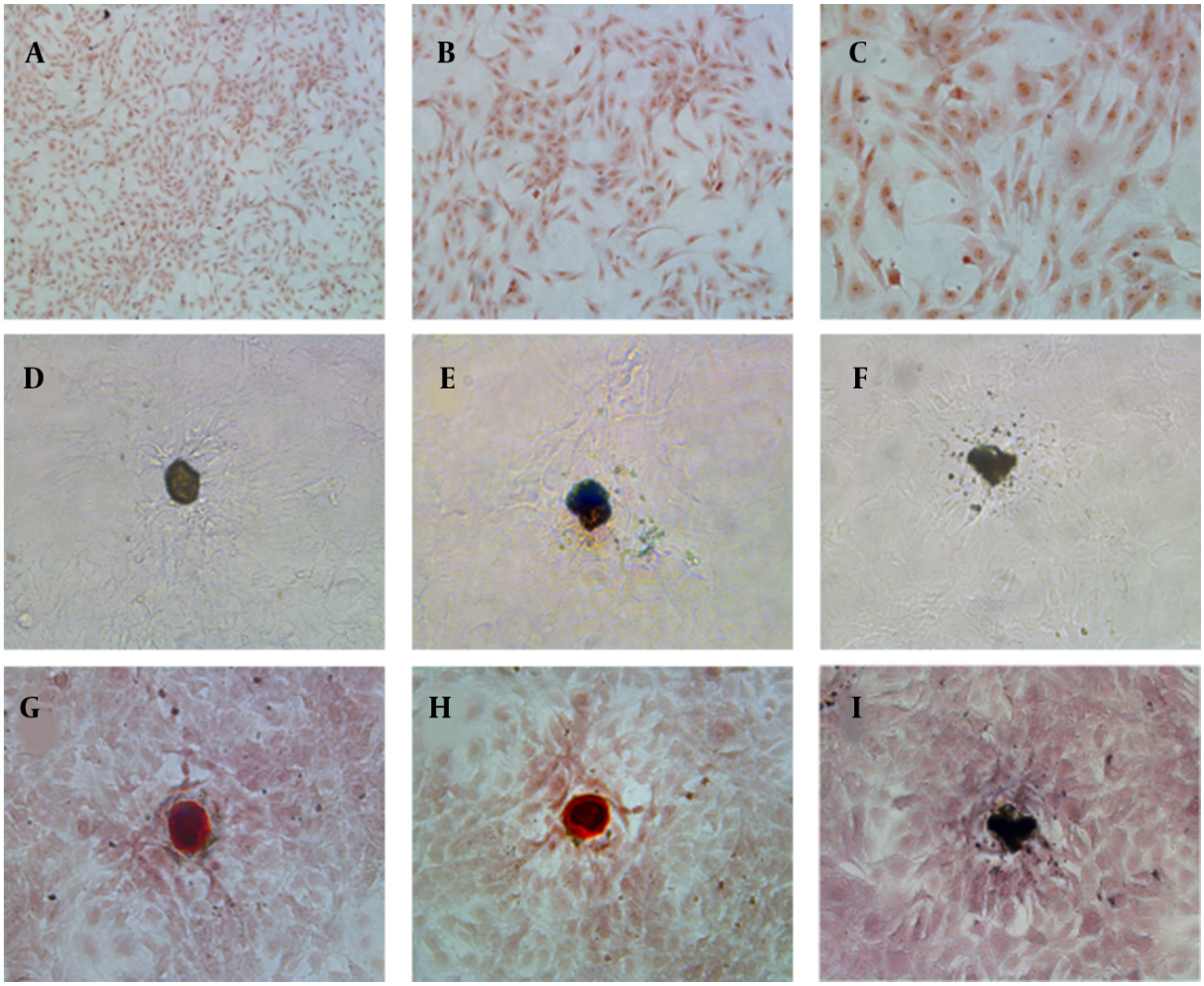

Figure 1. Characterizations of primary osteoblasts in culture: (A - C) Alkaline phosphatase histochemical staining of osteoblasts (10x, 20x, and 40x HE, respectively); (D - F) Osteoblasts calcified nodules before alizarin red S staining, 20x HE; (G - I) Alizarin red S staining of osteoblasts calcified nodules, 20x HE

Table 1. Ultraviolet-Visible Absorbance Values of Sephadex G-25

Wavelength (nm)	Blank	1	2	3	4	5	6	7	8	9	10	11	12
270	3.196	3.209	3.21	3.239	3.24	3.236	3.23	3.217	3.212	3.213	3.21	3.211	3.209
280	2.93	2.933	2.926	2.965	2.983	2.966	2.961	2.93	2.945	2.949	2.939	2.93	2.942
290	1.096	1.09	1.076	1.106	1.125	1.117	1.117	1.065	1.103	1.094	1.091	1.073	1.093
300	0.349	0.338	0.334	0.345	0.353	0.351	0.347	0.328	0.336	0.334	0.329	0.335	0.339
310	0.192	0.179	0.179	0.185	0.188	0.186	0.183	0.173	0.174	0.173	0.168	0.177	0.181
320	0.149	0.136	0.136	0.141	0.142	0.141	0.138	0.131	0.131	0.131	0.126	0.134	0.138

[a] $P < 0.05$ manifested statistical differences.

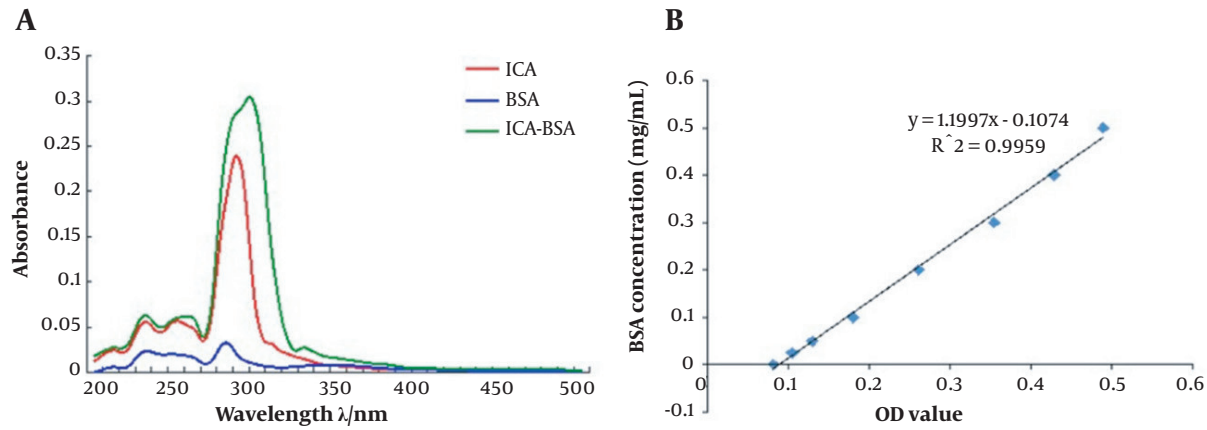

Figure 2. Sephadex G-25 chromatography results: (A) Ultraviolet (UV)-visible absorption curves of icariin (ICA), bovine serum albumin (BSA), and ICA-BSA; (B) UV absorbance of the standard curve by bicinchoninic acid

Table 2. The Proliferation of Osteoblasts Detected by MTT Assay

Group	Group A	Group B	Group C	Group D
OD value (mean ± SD)	0.89 ± 0.04	1.22 ± 0.11 [a]	0.42 ± 0.02	0.50 ± 0.05

[a] $P < 0.05$ manifested statistical differences.

Table 3. Cell Cycle Process Detected by Flow Cytometry

Group	A	B	C	D
G2 + S cycle (mean ± SD)	26.13 ± 1.06	31.71 ± 0.65 [a]	15.91 ± 2.88	15.96 ± 2.83

[a] $P < 0.05$ manifested statistical differences.

Table 4. Gray Values of Extracellular Signal-Regulated Kinase (ERK)1/2, Alpha-Tubulin, and Phospho (p)-ERK1/2 in the Cytoplasm of Osteoblasts

Group	α-Tubulin	Extracellular Signal-Regulated Kinase	Phospho-Extracellular Signal-Regulated Kinase
A	207887.40 ± 3056.95	379343.20 ± 2526.78	360607.20 ± 5741.25
B	207295.60 ± 3748.58	373522.40 ± 4376.59	437531.60 ± 3971.14
C	212214.60 ± 4624.37	379123.40 ± 3107.38	88348.00 ± 1312.26
D	210814.40 ± 4004.68	377202.60 ± 3171.07	64641.60 ± 3230.99

4.6. Icariin Improves Intracellular Calcium Ions Levels by Virtue of Fluo-3/AM

The concentration of intracellular calcium ions is important for the proliferation of cells. We employed Fluo-3/AM, a fluorescent probe, to label the intracellular calcium ions to determine whether ICA treatment could influence intracellular calcium ions. It was uncovered that osteoblasts in control groups exhibited similar low fluorescence intensity (Figure 4A-1 - D-1). However, ICA-BSA exposure significantly increased the Fluo-3/AM fluorescence intensity at 30 s (Figure 4A-2), suggesting that ICA-BSA stimulus led to calcium influx. However, the fluorescence intensity gradually declines, which might result from natural fluorescence quenching (Figure 4A-3). By contrast, a combination stimulus of ICA gave rise to slight enhancement in Fluo-3/AM fluorescence intensity at 30 s (Figure 4B-2) and gradually declined (Figure 4B-3). Notably, the fluorescence intensity was highly impeded after the addition of ICI18278 or PD98059 for 1 hour before or throughout the combination stimulus in comparison with combination exposure alone in 200 s (Figure 4C-2, C-3, D-2, and D-3). The above results also demonstrated the potential ability of ICA to promote the level of intracellular calcium ions in osteoblast cells (Figure 5).

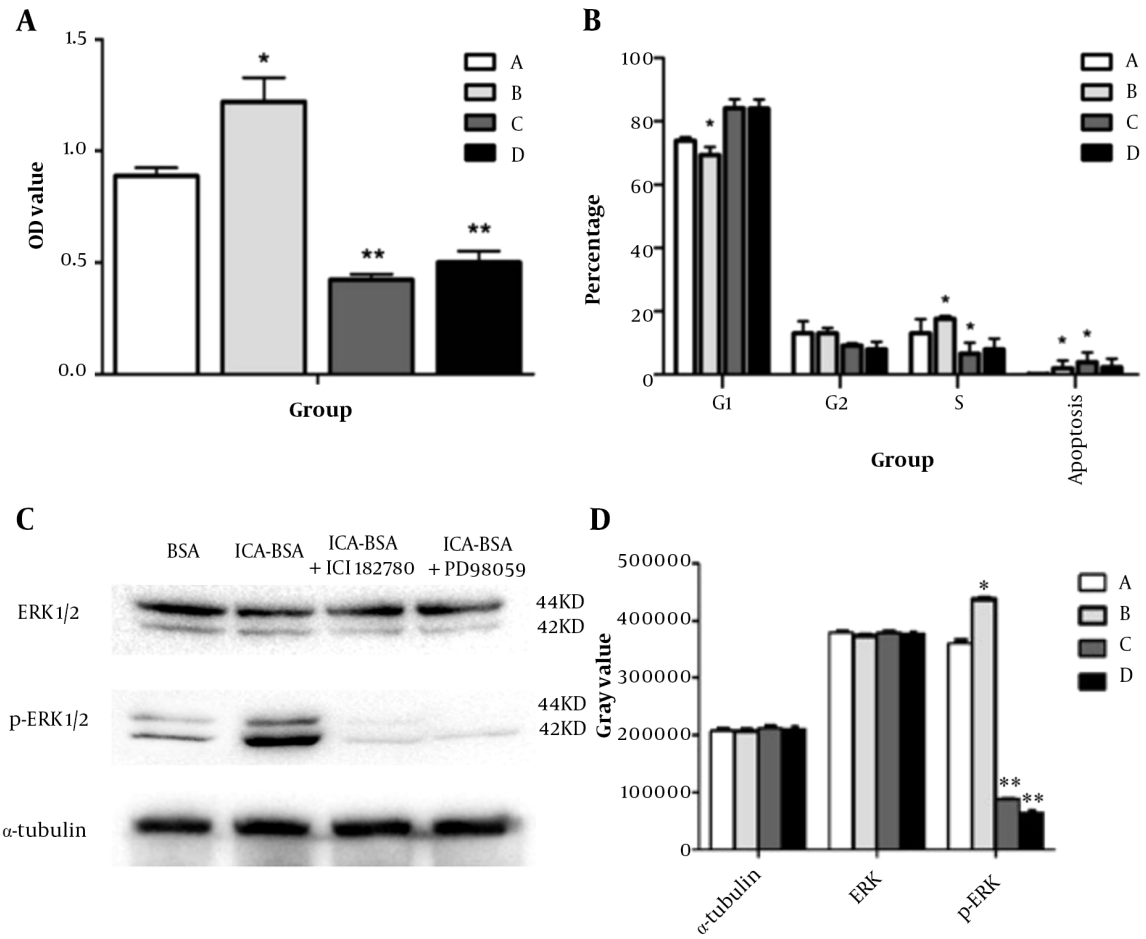

Figure 3. Non-nuclear effects of icariin affect osteoblast proliferation and signaling pathway activation: (A) The proliferation of osteoblasts in each group was detected by MTT assay. MTT results show that icariin (ICA)-bovine serum albumin (BSA) conjugate treatment (group B) significantly promoted the proliferation of osteoblasts compared with ICA (group A), ICA-BSA + ICI182780 (group C), and ICA-BSA + PD98059 (group D); (B) The cell cycle of osteoblasts in each group was detected by flow cytometry. Group A: ICA, group B: ICA-BSA, group C: ICA-BSA + ICI182780, group D: ICA-BSA + PD98059; (C) Protein expression levels of extracellular signal-regulated kinase (ERK)1/2 and phospho (p)-ERK1/2 in each group; (D) The relative expression levels of ERK1/2 and P-ERK1/2 proteins in each group. Group A: ICA, group B: ICA-BSA, group C: ICA-BSA + ICI182780 , group D: ICA-BSA + PD98059, * $P < 0.05$, ** $P < 0.01$

5. Discussion

As a major protein in blood plasma, serum albumin can transport various ligands to specific sites, both exogenous and endogenous (15). Understanding the interaction between proteins and small molecules would greatly promote deciphering the underlying mechanism (16). Bovine serum albumin, one of the serum albumin most diffusely researched, is highly structural homologous with human serum albumin (17, 18), so it is continually adopted in biophysics and biochemical research, and BSA can bind to many small molecules from different categories, including dyes, drugs, and toxic chemicals (19-21). As a result, there are increasingly clinical and experimental studies to discuss the transport, distribution, and metabolism of target molecules when bound to BSA.

Icariin, a small molecule substance, can easily pass through the cell membrane. However, when it is bound to BSA, the active structure of ICA is still kept, and the permeable membrane is prevented. Our results showed that stable ICA-BSA complexes could be formed by binding ICA to BSA. According to an analysis of thermodynamic quantities, hydrophobic forces are a significant player in the process (22). Hydrogen bonding interaction and van der Waals forces were the major interaction and forces between ICA and BSA. Ultraviolet/visible absorption is widely used to investigate protein structure changes and the formation of protein complexes. The absorption spectra of a

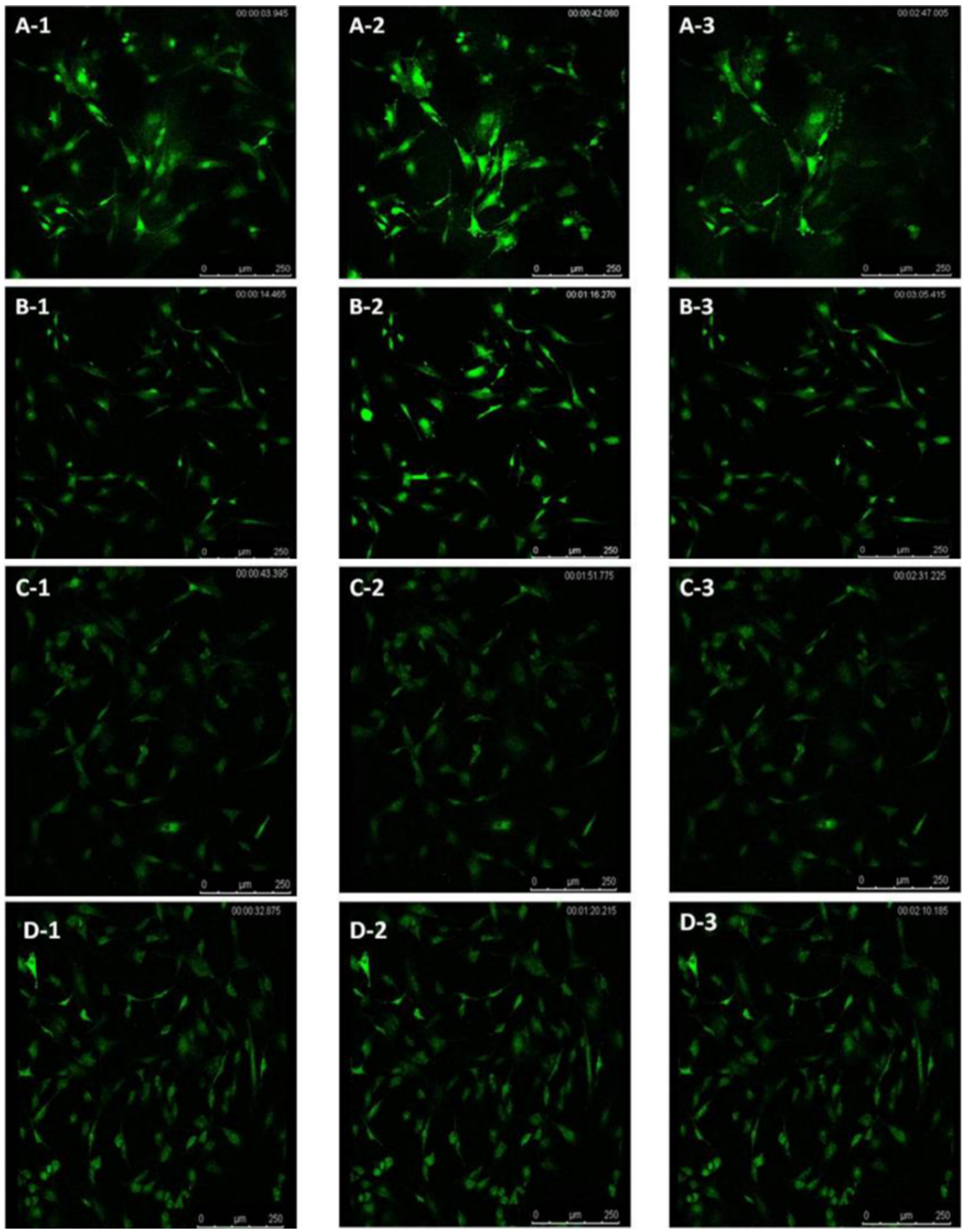

Figure 4. Fluo-3/AM fluorescence intensity changes in osteocytes of different compositions at different time points before and after icariin (ICA) or ICA-bovine serum albumin (BSA) addition. Group A: ICA, group B: ICA-BSA, group C: ICA-BSA + ICI182780, group D: ICA-BSA + PD98059

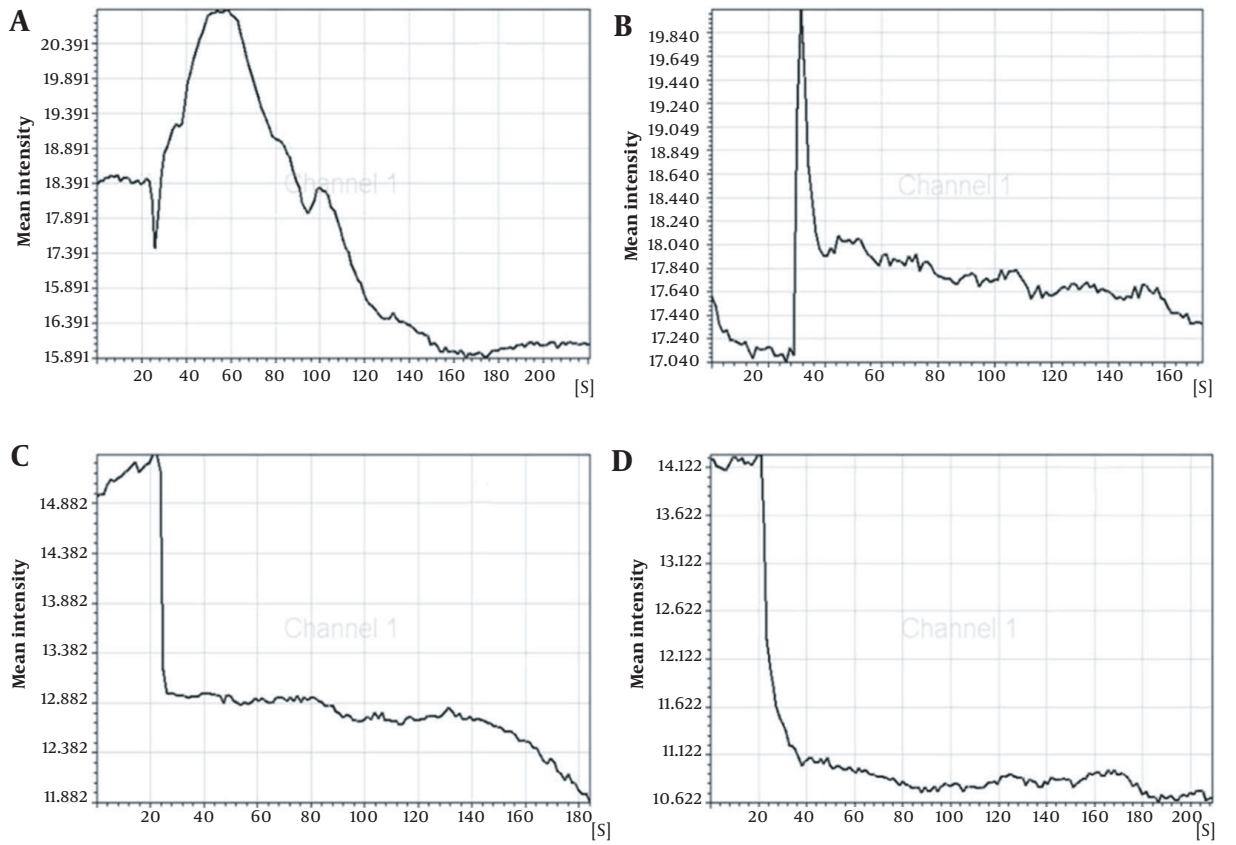

Figure 5. Intracellular Ca^{2+} fluctuations in tetrad osteocytes. Group A: Icariin (ICA), group B: ICA-bovine serum albumin (BSA), group C: ICA-BSA + ICI182780, group D: ICA-BSA + PD98059

particular protein are sensitive to the microenvironment surrounding the chromophores. Ultraviolet spectroscopy, essentially, is the technology most utilized to sense alterations in the local environment of fluorophores since it is susceptible, reproducible, and convenient. For this reason, ultraviolet spectroscopy is applicable to investigating the interaction between ICA-BSA complexes. Herein, we researched the binding of ICA to BSA with the ultraviolet spectrophotometry method and demonstrated that BSA displayed a powerful fluorescence emission peak at 282 nm, while that of ICA was at 291 nm and ICA-BSA at 305 nm, respectively. These results implied that ICA is bound to BSA. Therefore, BSA was bounded with ICA, resulting in conformational changes and a high probability of energy transfer between BSA and ICA. Ultraviolet/visible absorption spectra indicated the formation of BSA-ICA complexes.

It has been shown that protease can be purified from fresh chicken wing leaves by DEAE-Sepharose and Sephadex G-75 chromatography (23). Another study described and tested a method for isolating ring cells using an immunosorbent based on Sephadex G-75. The protein antigen (BSA) is covalently attached to the surface of the gel particles oxidized by sodium periodate (24). Sephadex G-25 has been widely used to purify various kinds of natural products; however, whether it could be used to isolate ICA-BSA remains to be determined. In this study, we applied Sephadex G-25 column chromatography to isolate and purify ICA-BSA to improve purification efficiency and reduce/avoid safety problems. Therefore, the Sephadex G-25 column represented a simplified and efficient method for purifying the ICA-BSA complex.

Icariin could prevent bone loss and bone deterioration caused by estrogen deficiency (25). It could directly influence osteoblastic cell proliferation and differentiation. These studies suggested that icariin might function as a selective estrogen in bone. Our present study indicated that icariin was most active at the concentration of 10 μg/L for its actions on both proliferation and differentiation of the cells. Furthermore, we found that icariin acted on osteoblasts partially through the ERK/MAPK signaling path-

way, synergically with estrogen receptor signaling. The role of estrogen at cellular levels is managed by estrogen receptors (ERs), and the binding of estrogen resulted in the binding of ERs to estrogen response elements (EREs) in the promoters of target genes and altering gene transcription (26). Estrogen receptors α and β are mainly present in the cytoplasm and nucleus and are slightly expressed on cell membranes (27). The cytoplasmic estrogen-ER complexes were translocated to the nucleus. They interacted with NF-κB, AP-1, SP-1, and other transcription factors to influence the transcription of target genes (28), which mediated the long-term role of estrogen. Alternatively, estrogen can trigger rapid effects by virtue of membrane-bound ERs. Many studies have demonstrated that estrogen can promote the proliferation and survival of cells (including Hela cells and MCF-7 cells) through ERK. Our results showed that ER signaling inhibitors (androgen receptor signaling inhibitors) inhibited the proliferation and differentiation of osteoblasts. The above data suggest that the role of icariin in osteoblasts is partially managed by signaling ERs.

In the present study, we probed into the actions of icariin and ICA-BSA on the MAPK signaling pathway. The results showed that ICA-BSA exposure could promote osteoblastic proliferation compared with the ICA group, and its effect could be blocked by ERK signaling pathway inhibitor, which indicated that the ERK signaling pathway was involved in icariin-induced osteoblastic proliferation. Recent studies have manifested that icariin can stimulate bone morphogenetic protein (BMP) and Runx-2, vital factors affecting osteoblastic differentiation and activity, to express in MC3T3 cells (29). In addition, it is known that BMP signaling pathway is associated with MAPK pathway in osteoblasts (30), in agreement with this study. The downstream substrates were phosphorylated, and nuclear transcription factors were eventually activated, mediating the biological effects of MAPKs. Most of these transcription factors participate in the proliferation of various cells directly. Icariin-bovine serum albumin treatment significantly triggered ERK to be phosphorylated and activated, while p-MEK1 inhibitor PD98059 and estrogen inhibitor ICI182780 suppressed ICA-induced ERK activation. These data further support the involvement of ERK signaling in icariin-induced intracellular signaling. To sum up, our results suggested that icariin could speed up osteoblasts' proliferation and differentiation by activating the ERK-MAPK pathway. In addition, it has also been suggested that icariin, a phytoestrogen, could activate classical ER signaling pathways or synergize with non-classical estrogen pathways. These findings render a view of the role of icariin in osteoblasts' proliferation and differentiation and might eventually benefit the clinical treatment of osteoporosis.

The regulation of the cell cycle plays a critical role in the proliferation and apoptosis of cells. Apoptosis may be triggered by cell cycle arrest, while the accelerated process leads to excessive proliferation and tumorigenesis. Our data uncovered that the stimulus of ICA-BSA contributed to the visibly elevated number of cells in the S and G2/M phases compared with the other groups, manifesting that ICA-BSA appeared to promote the cell cycle process. The concentration of intracellular calcium ions exhibits a close association with cell proliferation. However, the potential actions of ICA on cycle protein expressions and cell cycle processes in osteoblasts are rarely reported. The labeling of intracellular calcium ions was done using the fluorescent probe Fluo-3/AM to probe into the influence of ICA on the level of intracellular calcium ions. The osteoblasts in normal culture conditions showed low fluorescence intensity. However, ICA-BSA exposure gave rise to an observable enhancement in Fluo-3/AM fluorescence intensity, demonstrating that this stimulus can trigger cell proliferation. Markedly, in contrast with the combination stimulus alone, the fluorescence intensity was prominently repressed after ICI18278 or PD98059 addition for 1 hour before and throughout the combination stimulus. The above results also manifested the potential of ICA to promote the level of intracellular calcium ions in osteoblast cells.

5.1. Conclusions

In this study, icariin was first coupled with BSA. Since BSA macromolecules could not enter the cell through the lipid bilayer membrane, the interaction between icariin and BSA was mainly hydrophobic. Icariin-bovine serum albumin can retain the active structure of icariin well, so ICA-BSA can only bind to the estrogen receptor on the membrane so that the non-nuclear effect of icariin can be better studied. In addition, we found that through a rapid non-genomic ER signaling pathway independent of ligand and ERE and mediated by MAPK, icariin plays an estrogenic role in osteoblasts, providing a theoretical basis for the clinical search for icariin anti-osteoporosis pharmacological targets.

Footnotes

Authors' Contribution: Study concept and design: Weiqing Qian; acquisition of data: Dapeng Zhang, Yan Su; analysis and interpretation of data: Qiang He, Yajie Zhang, Ning Gu, Xu Zhang, Kun Yan, Nianwei Yao; drafting of the manuscript: Dapeng Zhang, Yan Su; critical revision of the manuscript for important intellectual content: Qiang He, Yajie Zhang, Ning Gu, Xu Zhang, Kun Yan, Nianwei Yao; statistical analysis: Qiang He, Yajie Zhang, Ning Gu, Xu Zhang,

Kun Yan, Nianwei Yao; Dapeng Zhang and Yan Su are co-first authors of the manuscript.

Conflict of Interests: All of the authors have no conflicts of interest to declare.

Data Reproducibility: The dataset presented in the study is available on request from the corresponding author during submission or after publication.

Ethical Approval: The animal study was checked and approved by the Animal Care Committee of the Nanjing University of Chinese Medicine and performed as per the Declaration of the National Institutes of Health Guide for Care and Use of Laboratory Animals (NIH publication NO.85-23, revised 1996).

Funding/Support: This work was supported by the National Natural Science Foundation of China (No. 30872726).

References

1. Mishra BH, Mishra PP, Mononen N, Hilvo M, Sievanen H, Juonala M, et al. Lipidomic architecture shared by subclinical markers of osteoporosis and atherosclerosis: The Cardiovascular Risk in Young Finns Study. *Bone*. 2020;**131**:115160. doi: 10.1016/j.bone.2019.115160. [PubMed: 31759205].
2. Kotrych D, Dziedziejko V, Safranow K, Sroczynski T, Staniszewska M, Juzyszyn Z, et al. TNF-alpha and IL10 gene polymorphisms in women with postmenopausal osteoporosis. *Eur J Obstet Gynecol Reprod Biol*. 2016;**199**:92–5. doi: 10.1016/j.ejogrb.2016.01.037. [PubMed: 26914399].
3. Mallarkey G, Reid DM. Osteoporosis therapeutics: recent developments at ASBMR. *Ther Adv Musculoskelet Dis*. 2016;**8**(1):3–7. doi: 10.1177/1759720X15623489. [PubMed: 26834845]. [PubMed Central: PMC4707418].
4. Wang C, Meng H, Wang X, Zhao C, Peng J, Wang Y. Differentiation of Bone Marrow Mesenchymal Stem Cells in Osteoblasts and Adipocytes and its Role in Treatment of Osteoporosis. *Med Sci Monit*. 2016;**22**:226–33. doi: 10.12659/msm.897044. [PubMed: 26795027]. [PubMed Central: PMC4727494].
5. Lazrak A, Yu Z, Doran S, Jian MY, Creighton J, Laube M, et al. Up-regulation of airway smooth muscle calcium-sensing receptor by low-molecular-weight hyaluronan. *Am J Physiol Lung Cell Mol Physiol*. 2020;**318**(3):L459–71. doi: 10.1152/ajplung.00429.2019. [PubMed: 31913654]. [PubMed Central: PMC7099432].
6. Xu T, Wang L, Tao Y, Ji Y, Deng F, Wu XH. The Function of Naringin in Inducing Secretion of Osteoprotegerin and Inhibiting Formation of Osteoclasts. *Evid Based Complement Alternat Med*. 2016;**2016**:8981650. doi: 10.1155/2016/8981650. [PubMed: 26884798]. [PubMed Central: PMC4738947].
7. Xu Y, Li L, Tang Y, Yang J, Jin Y, Ma C. Icariin promotes osteogenic differentiation by suppressing Notch signaling. *Eur J Pharmacol*. 2019;**865**:172794. doi: 10.1016/j.ejphar.2019.172794. [PubMed: 31733213].
8. Hsieh TP, Sheu SY, Sun JS, Chen MH, Liu MH. Icariin isolated from Epimedium pubescens regulates osteoblasts anabolism through BMP-2, SMAD4, and Cbfa1 expression. *Phytomedicine*. 2010;**17**(6):414–23. doi: 10.1016/j.phymed.2009.08.007. [PubMed: 19747809].
9. Pham CV, Pham TT, Lai TT, Trinh DC, Nguyen HVM, Ha TTM, et al. Icariin reduces bone loss in a Rankl-induced transgenic medaka (Oryzias latipes) model for osteoporosis. *J Fish Biol*. 2021;**98**(4):1039–48. doi: 10.1111/jfb.14241. [PubMed: 31858585].
10. Zuo S, Zou W, Wu RM, Yang J, Fan JN, Zhao XK, et al. Icariin Alleviates IL-1beta-Induced Matrix Degradation By Activating The Nrf2/ARE Pathway In Human Chondrocytes. *Drug Des Devel Ther*. 2019;**13**:3949–61. doi: 10.2147/DDDT.S203094. [PubMed: 31819369]. [PubMed Central: PMC6876636].
11. Qian WQ, Yin H, Sun HT. [Influence of different concentrations of Icariin on osteoblast metablism of rats]. *China Medical Herald*. 2011;**8**:23–5. Chinese.
12. Yang SH, Sharrocks AD, Whitmarsh AJ. MAP kinase signalling cascades and transcriptional regulation. *Gene*. 2013;**513**(1):1–13. doi: 10.1016/j.gene.2012.10.033. [PubMed: 23123731].
13. Chau JF, Leong WF, Li B. Signaling pathways governing osteoblast proliferation, differentiation and function. *Histol Histopathol*. 2009;**24**(12):1593–606. doi: 10.14670/HH-24.1593. [PubMed: 19795357].
14. Ho MX, Poon CC, Wong KC, Qiu ZC, Wong MS. Icariin, but Not Genistein, Exerts Osteogenic and Anti-apoptotic Effects in Osteoblastic Cells by Selective Activation of Non-genomic ERalpha Signaling. *Front Pharmacol*. 2018;**9**:474. doi: 10.3389/fphar.2018.00474. [PubMed: 29867480]. [PubMed Central: PMC5958194].
15. Leboffe L, di Masi A, Polticelli F, Trezza V, Ascenzi P. Structural Basis of Drug Recognition by Human Serum Albumin. *Curr Med Chem*. 2020;**27**(30):4907–31. doi: 10.2174/0929867326666190320105316. [PubMed: 30894098].
16. Zhu Y, Li B, Yin H, Ge S, Yu J. Analysis of the interaction of a new series of rhodanine derivatives with bovine serum albumin by fluorescence quenching. *Monatsh Chem*. 2013;**145**(1):167–73. doi: 10.1007/s00706-013-0991-x.
17. Liu S, Guo C, Guo Y, Yu H, Greenaway F, Sun MZ. Comparative binding affinities of flavonoid phytochemicals with bovine serum albumin. *Iran J Pharm Res*. 2014;**13**(3):1019–28. [PubMed: 25276204]. [PubMed Central: PMC4177624].
18. Dawoud Bani-Yaseen A. Spectrofluorimetric study on the interaction between antimicrobial drug sulfamethazine and bovine serum albumin. *J Lumin*. 2011;**131**(5):1042–7. doi: 10.1016/j.jlumin.2011.01.019.
19. Boehmler DJ, O'Dell ZJ, Chung C, Riley KR. Bovine Serum Albumin Enhances Silver Nanoparticle Dissolution Kinetics in a Size- and Concentration-Dependent Manner. *Langmuir*. 2020;**36**(4):1053–61. doi: 10.1021/acs.langmuir.9b03251. [PubMed: 31902212].
20. Molina-Bolívar JA, Galisteo-González F, Carnero Ruiz C, Medina-O´ Donnell M, Parra A. Spectroscopic investigation on the interaction of maslinic acid with bovine serum albumin. *J Lumin*. 2014;**156**:141–9. doi: 10.1016/j.jlumin.2014.08.011.
21. Xu X, Zhao M, Han Q, Wang H, Zhang H, Wang Y. Effects of piceatannol on the structure and activities of bovine serum albumin: A multi-spectral and molecular modeling studies. *Spectrochim Acta A Mol Biomol Spectrosc*. 2020;**228**:117706. doi: 10.1016/j.saa.2019.117706. [PubMed: 31753657].
22. Jattinagoudar L, Meti M, Nandibewoor S, Chimatadar S. Evaluation of the binding interaction between bovine serum albumin and dimethyl fumarate, an anti-inflammatory drug by multispectroscopic methods. *Spectrochim Acta A Mol Biomol Spectrosc*. 2016;**156**:164–71. doi: 10.1016/j.saa.2015.11.026. [PubMed: 26688208].
23. Serge NE, Laurette Blandine MK, Kumar S, Clerge T, Vijayalakshmi M. Extraction, purification, and biochemical characterization of serine protease from leaves of Abrus precatorius. *Prep Biochem Biotechnol*. 2017;**47**(10):1016–24. doi: 10.1080/10826068.2017.1373289. [PubMed: 28857663].
24. Fuks BB, Khazanova IV, Yurin VL. Separation of rosette-forming cells with the aid of an immunosorbent based on sephadex G-25 and G-75. *Bull Exp Biol Med*. 1975;**77**(7):792–4. doi: 10.1007/BF00799322. [PubMed: 1090313].
25. Zhu HM, Qin L, Garnero P, Genant HK, Zhang G, Dai K, et al. The first multicenter and randomized clinical trial of herbal Fufang for treatment of postmenopausal osteoporosis. *Osteoporos Int*. 2012;**23**(4):1317–27. doi: 10.1007/s00198-011-1577-2. [PubMed: 21505910].
26. Marino M, Pellegrini M, La Rosa P, Acconcia F. Susceptibility of estrogen receptor rapid responses to xenoestrogens: Physiological out-

comes. *Steroids*. 2012;**77**(10):910–7. doi: 10.1016/j.steroids.2012.02.019. [PubMed: 22410438].
27. Lorenzo J. A new hypothesis for how sex steroid hormones regulate bone mass. *J Clin Invest*. 2003;**111**(11):1641–3. doi: 10.1172/JCI18812. [PubMed: 12782664]. [PubMed Central: PMC156115].
28. Matsushita T, Chan YY, Kawanami A, Balmes G, Landreth GE, Murakami S. Extracellular signal-regulated kinase 1 (ERK1) and ERK2 play essential roles in osteoblast differentiation and in supporting osteoclastogenesis. *Mol Cell Biol*. 2009;**29**(21):5843–57. doi: 10.1128/MCB.01549-08. [PubMed: 19737917]. [PubMed Central: PMC2772724].
29. Cao H, Ke Y, Zhang Y, Zhang CJ, Qian W, Zhang GL. Icariin stimulates MC3T3-E1 cell proliferation and differentiation through up-regulation of bone morphogenetic protein-2. *Int J Mol Med*. 2012;**29**(3):435–9. doi: 10.3892/ijmm.2011.845. [PubMed: 22109711].
30. Kong XH, Niu YB, Song XM, Zhao DD, Wang J, Wu XL, et al. Astragaloside II induces osteogenic activities of osteoblasts through the bone morphogenetic protein-2/MAPK and Smad1/5/8 pathways. *Int J Mol Med*. 2012;**29**(6):1090–8. doi: 10.3892/ijmm.2012.941. [PubMed: 22426655].